

Structure of Concentrated HCl Solutions

Noam Agmon[†]

Department of Physical Chemistry and the Fritz Haber Research Center, The Hebrew University, Jerusalem 91904, Israel

Received: March 5, 1997; In Final Form: October 14, 1997[⊗]

A pentagonal ring is suggested as the basic structural unit of HCl(H₂O)₆ and (HCl)₂(H₂O)₆ in solution. Modeled after the X-ray structure of a caged H₁₃O₆⁺ compound, it contains bridged H₅O₂⁺ and Cl⁻ ions, each with a coordination number around four. In the most concentrated HCl solutions, one of the ligands solvating Cl⁻ is HCl, giving rise to a bichloride moiety. The proposed structure explains qualitatively the stoichiometry, ion mobility, (IR, Raman) spectroscopy and (X-ray, neutron) diffraction data of concentrated HCl solutions and provides a semiquantitative fit to the X-ray radial distribution function. The ring structure is a likely candidate for the structure of protonated HCl clusters in the gas phase and for the contact ion-pair formed following HCl dissociation in solution.

I. Introduction

Hydrochloric acid dissolves in liquid water up to a 1:3 mole ratio.¹ Similar stoichiometric restrictions do not hold in HCl crystals.² The crystal structure of the monohydrate,³ dihydrate,⁴ trihydrate,⁵ and hexahydrate⁶ have all been characterized by X-ray diffraction. In contrast, protonated water clusters seem to require a minimum of about 12 water molecules to solvate one HCl molecule.⁷

If HCl is fully dissociated in liquid water, both proton and chloride must be solvated with as little as three water molecules. How do such few water molecules solvate both ions? It is logical to assume that this requires special hydrogen-bonded structures, with water molecules being shared in the coordination shells of both ions. However, in spite of the information gleaned from X-ray and neutron diffraction measurements of aqueous HCl solutions over a wide composition range,^{8–13} these structures evaded determination. Most notable is the work of Triolo and Narten,⁹ who have interpreted the radial distribution function (RDF) in terms of isolated H₃O⁺ and Cl⁻ ions, with a hydration shell of four water molecules each. Such structures, requiring more than eight water molecules per HCl, are not satisfying models for concentrated HCl solutions.

In an effort to explain these stoichiometric restrictions, a structure involving direct contact between H₃O⁺ and Cl⁻ was postulated.^{14,15} While the through-space interaction is electrostatically favorable, the suggested structure requires an extremely bent hydrogen bond. As we shall see, this structure is inconsistent with the X-ray and neutron diffraction data.

Current assignments also ignore spectroscopic evidence for possible involvement of a protonated water dimer, the H₅O₂⁺ ion, which follows from the great enhancement in polarizability of concentrated HCl solutions.^{14,16–18} The question of whether H₃O⁺ or H₅O₂⁺ is the correct structure for the aquated proton was the subject of heated discussions.^{19–22} Giguère argued²¹ that the observed O···O distance of 2.52 Å⁹ is too long for H₅O₂⁺, whereas it is about right for H₃O⁺. Unfortunately, RDF peaks can arise as averages of several atomic interactions (as we shall see below).

Ionic mobility measurements^{23,24} show that the abnormal proton mobility (by the Grotthuss mechanism²⁵) is completely abolished in concentrated HCl, where the “hydrodynamic” proton mobility becomes equal to that of the chloride ion. First, if abnormal mobility in water is related to rapid isomerization between H₃O⁺ and H₅O₂⁺,^{25–27} its cessation might indicate that one of the two structures has become considerably more stable than the other. Second, the fact that both proton and ion now share the same hydrodynamic diffusion coefficient indicates a rather tight ion-pair structure.

Given the confusion concerning the possible structure of concentrated HCl solutions, perhaps one could turn for help to the crystal structures. Interestingly, in crystals of hydrated HCl, both H₃O⁺ and H₅O₂⁺ were identified.² The monohydrate is H₃O⁺ Cl⁻,³ the dihydrate is H₅O₂⁺ Cl⁻,⁴ the trihydrate is H₅O₂⁺ Cl⁻·H₂O,⁵ and the hexahydrate is assigned to H₉O₄⁺Cl⁻·2H₂O.⁶ It thus appears that the crystal environment determines which form of the solvated proton is favored.

The crystal structures can be very helpful in assigning peaks in the RDF, because typical interatomic distances do not change drastically in going from crystals to solutions. As an example, typical O···Cl distances are 2.95 Å in H₃O⁺···Cl⁻,³ 3.01–3.10 Å for H₅O₂⁺···Cl⁻,^{4,5} and 3.07–3.13 Å for H₂O···Cl⁻ (Figure 4 in ref 5). From these numbers it seems that the 3.13 Å peak observed in the RDF of liquid HCl⁹ cannot be assigned to a direct H₃O⁺···Cl⁻ contact.^{14,15} The chloride is more likely solvated by an unprotonated water molecule.

In contrast to the interatomic distances, the crystal structures themselves are not likely to be observed in the liquid phase, since they reflect the cooperative crystal environment effect in minimizing the free energy. An exception might involve the serendipitous discovery of a H₁₃O₆⁺ cation encapsulated within a cage compound.²⁸ This X-ray structure, Figure 1a, is stabilized by hydrogen bonds to several cage chloride anions (not shown). It is an appealing model for a 1:6 HCl/water mixture. The present work aims to show that it indeed provides a consistent interpretation of liquid HCl data.

The basic structure is a pentagonal ring composed of four water molecules, one proton and one chloride anion. Two of the water molecules bind the proton to form H₅O₂⁺, whereas

[†] FAX: 972-2-6513742. E-mail: agmon@fh.huji.ac.il.

[⊗] Abstract published in *Advance ACS Abstracts*, December 1, 1997.

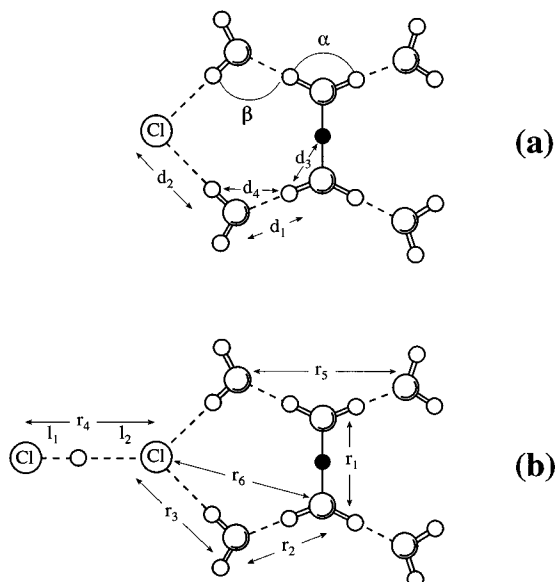


Figure 1. The suggested structural unit in mixtures of (a) 1:6 and (b) 1:3 HCl/water. Big and small circles represent O and H atoms, respectively, “the” H^+ atom is black. The indicated distances are estimated from X-ray and neutron diffraction data and are summarized in Table 3.

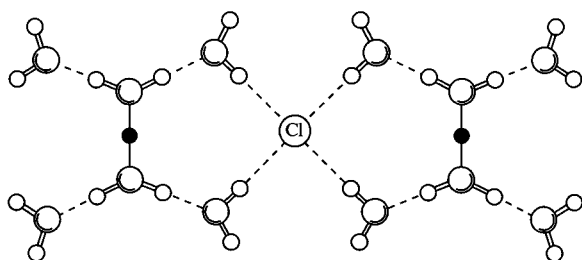


Figure 2. The structural unit(s) of Figure 1 may polymerize to complete the Cl^- hydration shell. The “dimer” shown (which, of course, is non-planar) includes two units from Figure 1a without one Cl^- . It is a suggestive structure for the product of solvating HCl in protonated gas-phase water clusters.⁷

the Cl^- resides between the other two. This structure is stabilized by a “through space” ionic interaction. Both H_5O_2^+ and Cl^- are solvated by four water molecules. The chloride solvation shell can be completed by polymerization, such as in Figure 2. Incidentally, this “dimer” (from which the second Cl^- has been deleted) might explain the required minimum of 12 water molecules for solvating HCl in protonated water clusters.⁷

Figure 1b explains the maximal 1:3 molar ratio obtained by forming a bichloride moiety, $(\text{ClHCl})^-$. Indeed, bichlorides present some of the strongest known hydrogen bonds in various crystal structures.²⁹ The bichloride has been identified in gas phase spectroscopy.³⁰ A tetrahedrally solvated $(\text{ClHCl})^-$ ion has been suggested as one of the (many) products of the reaction of gaseous HCl with anionic water clusters.³¹ Recent *ab initio* simulations have demonstrated its existence in liquid HCl.³²

It seems, therefore, that the proposed structures can explain the stoichiometry of concentrated aqueous HCl. The following sections demonstrate how these structures also explain the spectroscopy and, particularly, the diffraction data from concentrated HCl solutions.

II. Spectroscopy

Spectroscopic studies of concentrated aqueous HCl solutions point to the involvement of the protonated water dimer H_5O_2^+

rather than the protonated monomer H_3O^+ . Quantum chemistry calculations^{33,34} show that “the” proton in (isolated) H_5O_2^+ resides in a wide well in between the two oxygens, which are about 2.4 Å apart. Perturbations from the surrounding solvent can make one or the other oxygens momentarily more stable, causing the central proton to oscillate strongly between them.²⁷ This leads to high proton polarizability, as suggested by Zundel.¹⁶

There are three spectroscopic indications for such high protic polarizability: (a) In the IR-spectrum a broad continuum appears between 1000 and 3000 cm^{-1} , increasing in intensity at high acid concentrations.^{16,18} The continuum of vibrational states results from the fluctuating double-well potential of the proton along the O–H–O coordinate. (b) Depolarized Rayleigh scattering shows increasing scattering intensity with increasing HCl concentration assigned, again, to the easily polarizable H_5O_2^+ grouping.¹⁷ (c) The low-frequency Raman spectrum of water shows a peak near 180 cm^{-1} , assigned to $\text{H}_2\text{O}\cdots\text{HOH}$ hydrogen-bond stretch. It is completely depolarized at room temperature. With increasing $[\text{HCl}]$, the scattering intensity increases and becomes polarized, peaking in the isotropic spectrum at 206 cm^{-1} .^{14,15} Although Cl is a more polarizable atom than oxygen, Raman scattering from aqueous NaCl solutions shows a polarized peak at about 165 cm^{-1} , not near 206 cm^{-1} .¹⁵ The latter could therefore be assigned to H_5O_2^+ and its polarization attributed to protic (rather than electronic) polarizability.

In addition to the broad continuum, there are several discrete bands attributed to H_5O_2^+ vibrations.^{18,22} The 1710 and 1170 cm^{-1} bands were assigned to a water molecule bend and to the O–H–O asymmetric stretch within the H_5O_2^+ cation, respectively.¹⁸ These assignments have been criticized.^{19,21} Basically, the problem is that H_3O^+ may have intense IR bands at similar frequencies,³⁵ see Table 1. However, two arguments favor the H_5O_2^+ assignment: (a) The 1170 cm^{-1} band is IR active, but not Raman active.²² This could be understood if it is assigned to an antisymmetric mode. (b) A comparison with *ab initio* calculations,^{36,37} Table 1, shows that, by scaling the H_5O_2^+ frequencies to match experiment in the high frequency regime,³⁷ one obtains remarkable agreement with the liquid-phase data. In addition, the theory predicts that the asymmetric bending mode of H_3O^+ should appear at a slightly lower frequency than the water-bending mode in H_5O_2^+ . This refutes a claim by Giguère that 1710 cm^{-1} is too high for the bending mode of an “external” water molecule in the hypothetical H_5O_2^+ group.²¹

III. X-Ray Diffraction

X-ray is sensitive to electron density and will provide the X–X distances, X = O or Cl. In the X-ray RDF, one can typically identify nearest-neighbor and next nearest-neighbor X–X distances. In contrast, X–H and H–H distances are not observed by this technique, because of the low electron density of the hydrogen atoms. In addition to providing interatomic distances, there is valuable information in the width and amplitudes of the RDF peaks.

The classical X-ray data for liquid HCl are those of Triolo and Narten.⁹ Figure 3a shows the total intermolecular X-ray RDF for $\text{HCl}\cdot 4\text{H}_2\text{O}$ as obtained by digitizing Figure 4 of ref 9. It shows five peaks at 2.52, 3.13, 3.61, 4.15, and 4.60 Å. In comparison, X-ray scattering from liquid water shows a pronounced peak at 2.85 Å and a broad maximum around 4.6 Å, attributed to first and second nearest-neighbor water–water interactions in tetrahedral symmetry. However, direct assignment of peak positions to interatomic distances, r_i , may be

TABLE 1: Some Characteristic Vibrational Frequencies (in cm^{-1}) of Protonated Hydrates below 2000 cm^{-1} ^a

assignment ^b	H_5O_2^+			H_3O^+		
	experiment ^b	theory ^c C_2	theory ^c C_s	assignment ^b	experiment ^d	theory
OHO stretch (A)	1170 (IR)		1170	bend (S)	1100 (IR, R)	
water bend	1710 (IR, R)	1706	1750	bend (A)	1600 (IR, R)	1650 ^e

^a IR: Infra-Red active. R: Raman active. S: symmetric; A: asymmetric. ^b References 18 and 22. ^c Reference 37, scaled in comparison with experiment by original authors. ^d References 35 and 22. ^e MP2/6-311+ +G(2d,2p) calculation,³⁶ scaled as (1710/1777)1715.

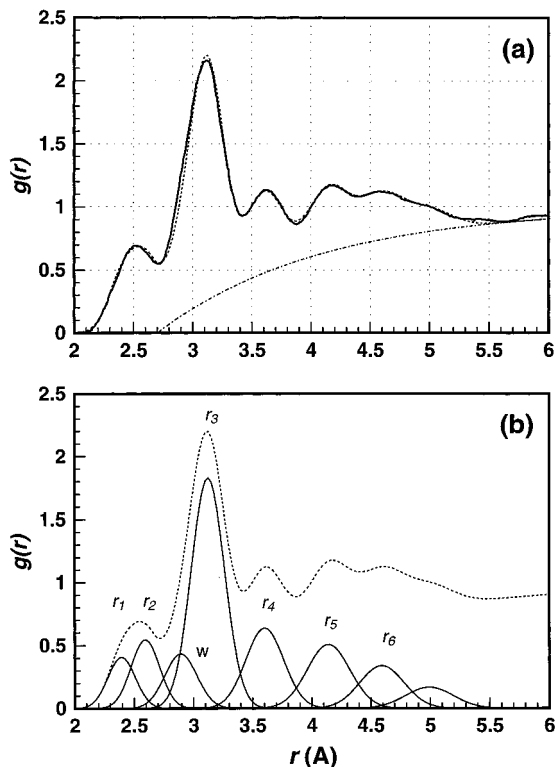


Figure 3. The radial distribution function obtained by X-ray scattering from $(\text{HCl})_{0.2}(\text{H}_2\text{O})_{0.8}$. (a) shows the experimental data (bold curve)⁹ with the fit to eq 5. The thin dotted line is the background scattering, eq 9, with $r_c = 2.7 \text{ \AA}$ and $r_e = 1.4 \text{ \AA}$. (b) shows the resolution into eight atom-atom interactions, $g_i(r)$, eq 8. Fitting parameters are collected in Table 2.

misleading because occasionally two pair interactions at similar distances may overlap to give a single peak. To separate these out, some RDF analysis is required.

In addition, important information may be conveyed by the number m_i of identical interatomic distances r_i within the postulated structural unit. Such “occupation numbers” may be useful in validating a suggested structure, but their determination requires a more quantitative RDF analysis. This analysis is never unambiguous,³⁸ but could nevertheless be informative, as seen below.

A. RDF Analysis. Let us consider two contributions to the total RDF, $g(r)$. One contribution is from a dominant, long-lived liquid structure unit such as that postulated in Figure 1. The other is an unstructured background density, $g_\infty(r)$, arising from numerous short-lived conformations for which no information is available. The structured part is further decomposed into a weighted sum of atom-pair distribution functions, $g_i(r)$. This allows one to estimate the number of equivalent interatomic distances of length r_i . The following derivation is based on standard material.^{38–42} It is produced in detail only because it is difficult to find in the present form.

Consider a “stoichiometric unit” (SU) of N atoms, with the same composition as the bulk solution. Its density is thus the bulk density, ρ_0 . Denote the (individual) atoms within the unit

by the index μ , where $\mu = 1, \dots, N$. The (individual) atoms of the solvent will be denoted by the index ν , where $\nu = 1, \dots, N, \dots, \infty$. Instead of counting atoms, one can count the different kinds of interactions. Each interaction generates an “equivalence class”. The i th class contains all interatomic distances (“bonds”) of average length r_i , between an atom of type A_i in the SU and another atom of type B_i in the liquid. For example, in the present work class $i = 3$ includes all $\text{O} \cdots \text{Cl}$ hydrogen-bonds peaking at 3.13 \AA . By definition, different classes are disjoint. One goal of the present section is to determine, from X-ray data, the number of elements in each class.

In a liquid, the interatomic distances are not fixed. Therefore, instead of having the distance between atoms μ and ν exactly $r_{\mu\nu}$, one introduces a probability density, $g_{\mu\nu}(r)$, for observing a separation r between these atoms. If atoms μ and ν are of types A_i and B_i (e.g., O and Cl) and their separation is r_i (e.g., 3.13 \AA) then $g_{\mu\nu}(r) \equiv g_i(r)$ [e.g., $g_3(r)$]. The pair distribution $g_i(r)$ is normalized so that

$$4\pi\rho_0 \int g_i(r) r^2 dr = 1 \quad (1)$$

namely, the probability of finding atom ν somewhere around atom μ is unity. Here $\rho_0 = 0.0323 \text{ molecule/\AA}^3$, the bulk density of a concentrated HCl solution [Table 1 in ref 9].

In the simplest case of an isotropic monoatomic liquid one may write^{41,42}

$$g(r) - g_\infty(r) = N^{-1} \sum_{\mu=1}^N \sum_{\nu \neq \mu} g_{\mu\nu}(r) = \sum_i n_i g_i(r) \quad (2)$$

The first form involves summation over atoms and the second, over all classes of pair interactions. The two representations must be equivalent.

Denote by $S_i(\mu)$ the set of (indices of) equivalent atoms in the liquid whose distance from atom μ is r_i . For example, if atom 2 is Cl and atom 6 is an oxygen atom whose distance from atom 2 is 3.13 \AA , then $6 \in S_3(2)$. If an atom μ does not contribute to the i th class, $S_i(\mu)$ will be empty. With this notation

$$n_i = N^{-1} \sum_{\mu=1}^N \sum_{\nu \in S_i(\mu)} 1 = \sum_{\nu \in S_i(\mu)} 1 \quad (3)$$

is the coordination number for the i th coordination shell. Indeed, if the SU is taken as a single atom, $N = 1$, the sum over μ reduces to a single term and n_i is the number of atoms in the set $S_i(\mu)$. If one selects a set of N atoms as the SU, the μ -sum produces N identical terms and n_i does not change.

Instead of counting the number of atoms in a specified shell around a given atom, one can count all equivalent distances r_i in which atoms from the SU participate. This arithmetic is more convenient for large heterogeneous SUs. Let us define the number of “bonds” m_i within an equivalence class such that when both relevant atoms are within the SU their interatomic distance counts once, whereas when μ is inside and ν outside

the SU, they contribute $1/2$ to m_i . With this convention

$$m_i = \sum_{\mu=1}^N \sum_{\nu \in S_i(\mu)} 1/2 \quad (4)$$

Since atom-pairs within the SU are counted twice by the double summation, each such pair indeed increments m_i by 1. Hence, with the above definition, $m_i = N n_i/2$.

When different kinds of atoms are involved, one should take into account the different atomic scattering factors f_μ . Since X-rays are scattered predominantly from electrons these factors, in the limit of forward scattering ($Q = 0$), are the total number of electrons associated with the relevant particle. Thus for water, including the two electrons from the hydrogens, $f_O = 10$. For chloride ion, including the negative charge, $f_{Cl} = 18$. Consequently, in the heteroatomic case, the intermolecular RDF is decomposed as^{9,40}

$$g(r) - g_\infty(r) = N \sum_{\mu=1}^N \sum_{\nu \neq \mu} f_\mu f_\nu g_{\mu\nu}(r) / (\sum_{\mu=1}^N f_\mu)^2 = \sum_i a_i g_i(r) \quad (5)$$

Again the sum over μ is restricted to the SU, whereas the ν -sum extends over the whole solvent. In general, The ratio $f_\mu f_\nu / (\sum_\mu f_\mu)^2$ depends more weakly on the scattering parameter Q than the individual f_μ 's. Hence taking the $Q = 0$ limit becomes a reasonable approximation. In the limit of identical f_μ 's, the scattering factors cancel and eq 5 reduces to 2.

We are interested in determining m_i from the weights a_i in the linear combination of interatomic RDFs. By restricting the ν -summation to the set $S_i(\mu)$, $g_{\mu\nu}(r)$ reduces to $g_i(r)$, whereas the factor $f_\mu f_\nu$ becomes independent of μ and ν . It depends only on the index i of the equivalence class. Suppose that this class involves an interaction between atoms A_i and B_i , then $f_\mu f_\nu = f_{A_i} f_{B_i}$. The sums are reordered as

$$\sum_i a_i g_i(r) = N \sum_i f_{A_i} f_{B_i} \sum_{\mu=1}^N \sum_{\nu \in S_i(\mu)} g_i(r) / (\sum_{\mu=1}^N f_\mu)^2 \quad (6)$$

Consequently, with the definition in eq 4

$$m_i = \left(\sum_{\mu=1}^N f_\mu \right)^2 a_i / (2N f_{A_i} f_{B_i}) \quad (7)$$

This allows one to obtain m_i by fitting $g(r)$ to a linear combination of pair interactions.

A useable model requires some functional form for $g_i(r)$ and $g_\infty(r)$. For the pair contribution, one usually assumes that either $g_i(r)$, $rg_i(r)$, or $r^2g_i(r)$ is a symmetric function of r . Following ref 43, we adopt the second assumption. Furthermore, if $rg_i(r)$ is a Gaussian, one has

$$g_i(r) = \frac{1}{4\pi r r_i \rho_0} \frac{\exp[-(r - r_i)^2 / 2\sigma_i^2]}{\sqrt{2\pi}\sigma_i} \quad (8)$$

Here σ_i is a width resulting from thermal fluctuations.

The background RDF describes an ensemble of short-lived and long-distance interactions. It is assumed to increase monotonically from zero at a cutoff distance, r_c , to unity at $r \rightarrow \infty$. This is depicted by the empirical function

$$g_\infty(r) = 1 - \exp[-(r - r_c)/r_{el}], \quad r > r_c \quad (9)$$

The parameter r_{el} could be interpreted as a characteristic decay

TABLE 2: Interatomic Parameters Obtained by Fitting the X-ray RDF of Concentrated HCl,⁹ Figure 3, to Equations 5 and 8^a

number	r_i (Å)	σ_i (Å)	a_i	m_i
1	2.40	0.115	0.27	1.8
2	2.60	0.12	0.45	3.0
w	2.90	0.135	0.50(0.75)	3.3
3	3.13	0.14	2.55(2.75)	9.5
4	3.61	0.16(0.19)	1.35(2.75)	3
5	4.15	0.18(0.20)	1.60(3.75)	11
6	4.60	0.185(0.21)	1.35(3.85)	5
	5.0	0.20(0.23)	0.85(4.5)	

^a Values in parentheses were obtained by neglecting the background density. The number of equivalent bonds within the stoichiometric unit m_i was calculated from a_i using eq 7 with $N = 10$, $f_O = 10$, and $f_{Cl} = 18$.

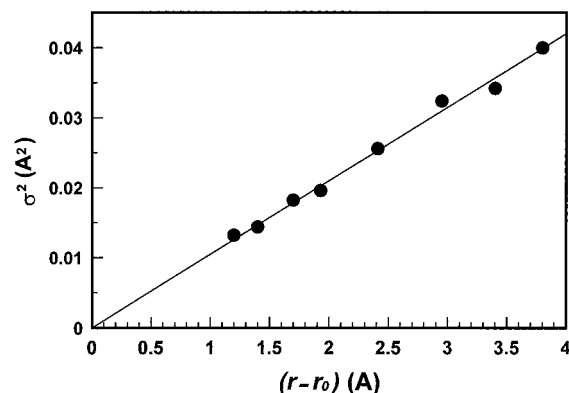


Figure 4. A correlation of rms deviations with interatomic distances for the fitting parameters of Table 2 (circles). The line is a fit to eq 10.

length for electronic correlations (on the order of 1 Å). The choice of $g_\infty(r)$ affects m_i the most, σ_i less, and r_i hardly at all.

In discussing the X-ray data from the most concentrated 1:4 solution studied,⁹ two water molecules should be added to the structure in Figure 1b. The SU then has $N = 10$ heavy atoms: eight H₂O and two HCl molecules. Using $f_O = 10$ and $f_{Cl} = 18$ gives $\sum_\mu f_\mu = 116$. The dashed curve in Figure 3a shows a fit to the experimental $g(r)$, which is the full curve there. The background RDF, $g_\infty(r)$, is depicted by the thin dotted line (assuming $r_c = 2.7$ Å and $r_{el} = 1.4$ Å). Eight inter-atomic interactions g_i were included. Their parameters are collected in Table 2. Given in parentheses are the values for these parameters from a fit (not shown) that assumes $g_\infty(r) \equiv 0$.

B. Structural Diffusion Model. Before discussing in detail the relation between the parameters r_i and m_i and the proposed structure, let us check that the widths σ_i of the various peaks vary in a physically reasonable manner. Figure 4 shows a nice linear correlation between σ_i^2 and r_i . It is interesting that, within the accuracy of the present analysis, the width for all X...X peaks (X = O or Cl) fall on the same line.

A linear correlation is indeed expected from the model of "structural diffusion",

$$\sigma_i^2 = c(r_i - r_0) \quad (10)$$

This model was originally applied to the different solvation shells in non hydrogen-bonded liquids.^{41,42,44} In the present case, r_i are nearest neighbor X-X distances within X...HO hydrogen-bonds. Thus, if r_0 depicts the OH bond length then $r_i - r_0$ is the corresponding hydrogen-bond length. We find that $r_0 = 1.2$ Å, which is the maximal OH bond length observed within the H₅O₂⁺ ion. The line through the origin in Figure 4 has $c = 0.0105$ Å.

TABLE 3: Intermolecular Distances (and Angles) for Concentrated HCl^e

distance or angle	this work	X-ray ^{b,c}	neutron			total ^c	cage structure ^e
			XX ^d	XH ^d	HH ^d		
$r_1(\text{O}\cdots\text{O})$	2.40 ^b		2.37				2.39
$r_2(\text{O}\cdots\text{O})$	2.60 ^b	2.52	?				2.52
$r_3(\text{O}\cdots\text{Cl})$	3.13 ^b	3.13	3.18			3.1 ^f	3.17
$r_4(\text{Cl}\cdots\text{Cl})$	3.61 ^b	3.61	?				
$r_5(\text{O}\cdots\text{O})$	4.15 ^b	4.15					?
$r_6(\text{O}\cdots\text{Cl})$	4.60 ^b	4.6					?
$d_1(\text{H}\cdots\text{O})$	1.59			1.69		1.6	
$d_2(\text{H}\cdots\text{Cl})$	2.15			2.14		2.1	
$d_3(\text{H}\cdots\text{H})$	1.98				2.02	2.1	
$d_4(\text{H}\cdots\text{H})$	2.09					2.1	
$l_1(\text{Cl}\cdots\text{H})$	1.6 (?)			1.69		1.6	
$l_2(\text{Cl}\cdots\text{H})$	2.0 (?)			2.14		2.1	
α	106°						132°(?)
β	106.5°						?

^aSee Figure 1 for their definition. ^bSee Table 2. ^cReference 9. ^dReference 13, fitted in Fourier space. ^eReference 28. ^fReference 10.

Figure 4 provides some justification for using a background density since, with $g_\infty(r) = 0$, the widths for the large r_i peaks (Table 2) fall above the line. The correlation also indicates that the 2.52 Å peak should be split between two interactions (at 2.4 and 2.6 Å). While it could be fitted with a single g_i , the required width would be 0.15 Å, significantly above the linear correlation of Figure 4.

C. Peak Assignment. The peak distances, r_i , are the primary information used in structure determination, since uncertainties in their values are much smaller than in the occupation numbers m_i . Problems arise when two peaks overlap, such as for g_1 and g_2 . In such cases one searches for additional evidence for the correctness of the assignment. The strategy of the following analysis is as follows. First the nearest-neighbor distances ($r_1 - r_4$) are discussed and compared with those observed in the cage structure²⁸ and in HCl-hydrate crystals.² Then second nearest-neighbors (r_5 and r_6) and occupation numbers (m_i) provide a check for the consistency of the assignments.

i. $r_1 = 2.4$ Å is in agreement with accurate quantum chemistry calculations for the O—O distance in H_5O_2^+ .³⁷ In the original X-ray work,⁹ the 2.52 Å peak has been assigned to a hydrogen-bond between water and H_3O^+ .^{9,14,21} The correlation shown in Figure 4 provides one indication that this peak is actually composed from two separate interactions at $r_1 = 2.4$ and $r_2 = 2.6$ Å. Additional evidence for this interpretation will be provided below.

ii. $r_2 = 2.6$ Å is assigned to the hydrogen-bond length to water ligands in the first hydration shell of H_5O_2^+ . *Ab initio* calculations for small protonated hydrates show a larger distance, around 2.73 Å,⁴⁵ whereas for the cage structure a smaller value of 2.52 Å has been reported.²⁸ Hydrogen-bond distances tend to decrease with increasing cluster size.⁴⁶ The value of 2.6 Å is in agreement with an analysis using the Pauling—BEBO correlation of intramolecular O—H bond lengths with intermolecular hydrogen-bond lengths.⁴⁷

iii. $r_3 = 2.13$ Å was convincingly assigned to O \cdots Cl interactions between water ligands and the Cl^- ion solvated by them.⁹ The same distance is found in studies of chloride salt solutions (see ref 9) and in the cage compound.²⁸ In HCl⁻ hydrate crystals [Figure 4 in ref 5], distances around 3.1 Å are observed for Cl^- solvated by H_2O , which drop to 3.00–3.05 Å when the chloride is bound to H_5O_2^+ . A direct bond between H_3O^+ and Cl^- is only 2.95 Å long,³ which rules out this possible interpretation¹⁴ for r_3 .

iv. $r_4 = 3.6$ Å is assigned here to the Cl \cdots Cl interaction in the bichloride ion, $(\text{ClHCl})^-$. Bihalides form strong hydrogen bonds,²⁹ the strongest being the bifluoride. Bichloride has been

identified in gas phase spectroscopy³⁰ as well as in solid matrices; however, it has not been previously identified in the liquid phase, except in recent *ab initio* simulations of aqueous HCl.³² Interestingly, neutron diffraction from fluid HCl (under pressure) shows a sharp peak in $g_{\text{ClCl}}(r)$ in the range 3.7–3.8 Å,⁴⁸ 3.6 Å is also twice the Cl^- crystal radius.²⁹

Quantum chemistry studies⁴⁹ indicate that an isolated bichloride can have either a short Cl—Cl distance around 3.15 Å, with a nearly symmetrical proton, or a longer 3.2–3.3 Å distance with an off-center hydrogen. The latter is better viewed as Cl^- solvation by a HCl molecule. In solution, additional water ligands around the chloride should lead to lengthening of the $\text{Cl}^- \cdots \text{HCl}$ bond and a decrease in its hydrogen-bond energy below the 20 kcal/mol gas-phase value. For this reason, the suggestion³² that the bichloride contributes to the 3.13 Å peak seems less convincing than its present assignment to $r_4 = 3.6$ Å.

Two alternative assignments for r_4 have appeared in the literature. Triolo and Narten ascribed the 3.61 Å peak to a direct $\text{Cl}^- \cdots \text{Cl}^-$ interaction.⁹ This unfavorable electrostatic arrangement has not been observed in recent simulations of concentrated HCl.³² Walrafen and Chu¹⁴ proposed direct contact between H_3O^+ and Cl^- at 3.13 Å with two secondary O \cdots Cl interactions with the first-shell water ligands of H_3O^+ at 3.61 Å. If this structure were correct, the latter peak should be stronger than the 3.13 Å peak, which in fact is the most intense feature in the RDF.

v. $r_5 = 4.15$ Å is shorter than the 4.6 Å second nearest-neighbor distance observed in neat water. If this distance is ascribed to the O \cdots O separation between the two water ligands which bind to H_5O_2^+ , Figure 1b, then

$$r_5 = 2r_2 \sin(\alpha/2) \quad (11a)$$

where the angle α is defined in Figure 1a.

The question is which value of α to adopt (Table 3). The cage structure has $\alpha = 132^\circ$.²⁸ This value seems questionable because (a) the two complementary angles there are 111° , so that the three angles do not sum up to 360° as they should for the planar geometry assumed;²⁸ (b) the water HOH angle, normally 104.5° , is not likely to exceed 120° in the protonated dimer. Accurate *ab initio* calculations for H_5O_2^+ have $\alpha \approx 109^\circ$.³⁷ This value tends to decrease in larger protonated hydrates to around 106° ,⁵⁰ the value adopted here.

Using $r_2 = 2.6$ Å and $\alpha = 106^\circ$ in eq 11a gives $r_5 = 4.15$ Å, in excellent agreement with the corresponding peak value from

Figure 3b. Its observation provides a second evidence for the H_5O_2^+ model.

vi. $r_6 = 4.6 \text{ \AA}$ is assigned to the second nearest-neighbor $\text{O}\cdots\text{Cl}$ interaction seen in Figure 1b. If β is the appropriate $\text{Cl}\cdots\text{O}\cdots\text{O}$ angle, Figure 1a, then

$$r_6^2 = r_2^2 + r_3^2 - 2r_2r_3 \cos(\beta) \quad (11b)$$

The angle β is adjusted to obtain the measured value of r_6 giving $\beta = 106.5^\circ$, slightly lower than the tetrahedral angle 109.5° . The reduction in β might be ascribed to ring strain. A consistency check on β would be provided by d_4 below.

D. Occupation Numbers. The amplitudes a_i of the atom-atom interactions, as obtained from eq 5, are summarized in Table 2. The number, m_i , of equivalent r_i bonds within the SU is then calculated using eq 7. This added information could help corroborate the proposed structure and indicate where the two additional water molecules are attached in the 1:4 HCl/water stoichiometry. Unfortunately, the m_i 's depend on the empirical background density $g_\infty(r)$. One can therefore expect only a semiquantitative determination of their values, particularly for the longer r_i 's.

The shortest intermolecular distances are within and around the H_5O_2^+ moiety. We find $m_1 = 1.8$ and $m_2 = 3$. Since $g_1(r)$ and $g_2(r)$ overlap considerably, a shift of intensity between them is consistent with $m_1 = 1$ and $m_2 = 4$, the values suggested by the structure in Figure 1b. The value of $m_w \approx 3$ could be understood if all the "dangling" hydrogens in the SU are hydrogen bonded to water molecules outside the SU, contributing half a bond each. The number of $\text{O}\cdots\text{Cl}$ hydrogen bonds, $m_3 = 9.5$, is in agreement with the earlier determination⁹ of a coordination number of 4.5 for each of the two chloride ions. If the structure polymerizes and the two additional water molecules are bound to the two chlorides, one obtains $m_3 = 6$. Since in recent neutron diffraction measurements¹³ a water coordination number of 3.5 was found for each chloride (corresponding to $m_3 = 7$), the agreement might be considered satisfactory. In contrast, $m_4 = 3$ disagrees with the present suggestion of a single $\text{Cl}\cdots\text{Cl}$ bond. Either the background subtracted is too small or else the observed peak at 3.6 \AA is too strong, as suggested from recent X-ray measurements.¹³

The number of second nearest-neighbors is even more ambiguous. The number of second nearest neighbor $\text{O}\cdots\text{O}$ distances in Figure 1b is 6, provided that all of them are roughly equivalent to r_5 . The high value of $m_5 = 11$ suggests that there should be quite a number of similar distances to oxygen atoms outside the SU. Finally, if the structure polymerizes, there should be four second nearest-neighbor $\text{O}\cdots\text{Cl}$ interactions within the SU, plus two half-interactions through the two additional water molecules which complete the hydration shell of the two chlorides. This explains the value of $m_6 = 5$ obtained in the present analysis.

IV. Neutron Diffraction

Neutron diffraction is sensitive to light atoms and will thus provide information on H-H and H-X interactions, which are unobservable using X-ray scattering. The measurements of Triolo and Narten⁹ provided only the total intermolecular $g(r)$. As HCl becomes progressively more concentrated, a peak at 2.2 \AA is replaced by two peaks, at 2.1 and 1.6 \AA .⁹ Recently, Kameda has used isotopic substitution to obtain the partial RDFs for X-X, H-X, and H-H interactions.¹³ The most prominent nearest-neighbor peaks are collected in Table 3. The X-X distances could be directly compared with the X-ray results.

From them, plus the angles α and β , one can predict the X-H and H-H distances. In this process, one makes use of three intramolecular O-H distances: (a) in bulk water, $r_{\text{OH}} = 0.98 \text{ \AA}$; (b) the four external OH bonds in H_5O_2^+ , $r'_{\text{OH}} = 1.01 \text{ \AA}$; and (c) the three OH bonds in H_3O^+ , $r''_{\text{OH}} = 1.04 \text{ \AA}$.^{12,45} Only nearest-neighbor distances within the ring (d_1 - d_4) or the bichloride moiety (l_1 and l_2) would be considered below.

A. $g_{\text{XX}}(r)$. (i) r_1 . g_{XX} reveals a peak at 2.37 \AA with a coordination number close to 1. This provides the most direct proof for the ultrashort $\text{O}\cdots\text{O}$ distance characterizing H_5O_2^+ .

(ii) r_2 . Of concern is the lack of a clear peak at 2.6 \AA , unless it is buried in the background.

(iii) r_3 . The peak at 3.18 \AA with a coordination number of 3.5 (i.e., $m_3 = 7$) is in agreement with its present assignment to $\text{O}\cdots\text{Cl}$ interactions.

B. $g_{\text{XH}}(r)$. (i) d_1 . The shortest observed X-H peak is at 1.69 \AA . The $\text{O}\cdots\text{H}$ hydrogen-bond length between H_5O_2^+ and its first-shell water ligands is given by

$$d_1 = r_2 - r'_{\text{OH}} \quad (12a)$$

Thus $d_1 = 1.59 \text{ \AA}$. (The corresponding $\text{H}\cdots\text{O}$ distance to H_3O^+ would be $2.52 - 1.04 = 1.48 \text{ \AA}$.) The observed interaction at 1.69 \AA could be a mixture of d_1 with the hydrogen-bond length between two water molecules $d_w = 1.85 \text{ \AA}$.

(ii) d_2 . d_2 is assigned to the $\text{H}\cdots\text{Cl}$ hydrogen bond between the ring chloride and its water ligand. Indeed

$$d_2 = r_3 - r_{\text{OH}} \quad (12b)$$

gives $d_2 = 2.15 \text{ \AA}$, in excellent agreement with observed value of 2.14 \AA . In comparison, the model of Walrafen and Chu¹⁴ produces $\text{Cl}\cdots\text{H}$ interactions at 2.86 \AA , where no peak is observed in the neutron diffraction.

(iii) l_1 and l_2 . Assuming linearity, these distances obey

$$l_1 + l_2 = r_4 \quad (12c)$$

For a symmetric bichloride, with the H atom in its center, one expects $l_1 = l_2 = 1.8 \text{ \AA}$. In a nonsymmetric bichloride the hydrogen is displaced 0.2 - 0.3 \AA from the center.⁴⁹ One might then expect $l_1 = 1.5$ - 1.6 \AA and $l_2 = 2.0$ - 2.1 \AA . In this case, l_1 and d_1 would contribute to the 1.6 \AA peak, whereas l_2 and d_2 contribute to the 2.2 \AA peak in g_{HX} . The present accuracy does not allow one to locate the bichloride proton.

C. $g_{\text{HH}}(r)$. $d_3 \approx d_4 = 2.0 \text{ \AA}$ is assigned to $\text{H}\cdots\text{H}$ interactions between neighboring water molecules in the ring. Using previously determined distances and angles (Table 3)

$$d_3^2 = (r_1/2)^2 + r_{\text{OH}}'^2 + r_1 r_{\text{OH}}' \cos(\alpha/2) \quad (12d)$$

$$d_4^2 = d_1^2 + r_{\text{OH}}'^2 - 2d_1 r_{\text{OH}}' \cos(\beta) \quad (12e)$$

gives $d_3 = 1.98 \text{ \AA}$ and $d_4 = 2.09 \text{ \AA}$, in agreement with the observed peak at 2.02 \AA .

The 2.1 \AA peak in the total RDF was initially assigned to $\text{Cl}\cdots\text{H}$ interactions. Since its intensity does not increase with HCl (actually, DCl) concentration, it was later reassigned to $\text{H}\cdots\text{H}$ interactions.⁹ In the present model, it is due to both $\text{H}\cdots\text{H}$ and $\text{Cl}\cdots\text{H}$ interactions at distances d_2 , d_3 , d_4 , and l_2 . It does not increase in intensity above the 1:6 HCl/water ratio, because additional HCl forms the bichloride bond. There is only one

interaction of type l_2 , compared with a total of 10 interactions of the other three types.

V. Perspective

Twenty-seven years after the first HCl diffraction data,⁸ a consistent assignment has been achieved. Concentrated HCl has a well-defined hydrogen-bonded ring structure connecting a H_5O_2^+ moiety with a Cl^- ion. In the most concentrated HCl solution considered, one of the water ligands in the chloride solvation shell is replaced by a HCl molecule, forming a (possibly non-symmetric) bichloride anion. The ring structure could further polymerize, giving rise to the high coordination numbers for the chloride ions.

The quantitative part of the analysis involves an empirical fit to the X-ray scattering data from concentrated HCl solutions.⁹ It applies a formula, eq 7, for the number m_i of equivalent r_i distances within a structural unit. The features in the RDF become sharper with increasing HCl concentration, indicating transition to a more ordered phase. The structure emerging gives rise to seven identifiable peaks into which the total RDF is resolved. With the aid of this structure, the peaks in the neutron diffraction partial RDFs¹³ could also be assigned.

The structure in $g(r)$ emerges on the background of the structureless $g_{\infty}(r)$. One might picture this background as arising from a multitude of transient solvent conformations which are either very short lived or of low probability. The structure (Figure 1) emerging from this seemingly chaotic ensemble, should not be confused with a static crystal structure, since the solvent is a dynamic entity. It rather represents a small set of conformations which are either sufficiently long lived or occur frequently enough to leave their mark on the scattering intensity.

The postulated ring-structure endows extra stability to the ion pair through a direct Coulomb interaction. The stability may be even larger for HF. Indeed, F is the most electronegative halogen and bifluoride forms the strongest known hydrogen bond.²⁹ If in HF such structures persist also at submaximal concentrations, they may be the key for solving the "HF riddle".²⁰ Why is HF such a weak acid in spite of indications that it is almost completely ionized? Strong ion pairing through structures such as in Figure 1b might be the answer.

The "ring ion pair" supposedly explains the loss of abnormal prototropic mobility in concentrated HCl, in which proton and Cl^- diffusion occurs at similar rates to that of water molecules. However, the mechanism of proton mobility under these conditions cannot involve simple ring translation, since the ring has zero net charge. Hence the mechanism of ionic mobility in concentrated acids is an interesting problem which is worth further investigation.

For less concentrated HCl (and possibly other acids), the structures of Figure 1 might represent a short-lived intermediate along the dissociation path. The contact ion pair sometimes postulated for acid dissociation in water could involve ring structures rather than linear structures, such as studied in ref 51. It would be interesting if such transient intermediates could be detected by time-resolved spectroscopy.⁵²

With regard to the debate concerning the "correct" form of protonated water,^{21,22} the present assignment identifies H_5O_2^+ as "the" form of protonated water at high HCl concentrations. However, in more dilute HCl solutions H_3O^+ could become the more stable cation.²⁰ While H_5O_2^+ requires only four water ligands for full solvation, localization of a proton on a single water molecule occurs only when all three water ligands in the first solvation shell are tetrahedrally coordinated.²⁵ This requires a complete second shell or 12 water molecules total, which could

explain the enhanced relative stability of H_3O^+ in dilute solutions. Nevertheless, assuming that the abnormal proton mobility in water results from rapid interconversion between the two cations,^{25,27} they should be nearly isoenergetic even in dilute acidic aqueous solutions.²⁶

Acknowledgment. I am grateful to Yasuo Kameda for sending me his neutron diffraction data prior to publication. I thank Shalom Baer, Avi Bino, James T. Hynes, Yasuo Kameda, Elise Kochanski, and Yitzhak Marcus for correspondence and discussions. Work supported in part by a grant from the Israel Science Foundation. The Fritz Haber Research Center is supported by the Minerva Gesellschaft für die Forschung, München, FRG.

References and Notes

- (1) Gerrard, W. *Chem. Ind. (London)* **1969**, 295.
- (2) Lundgren, J.-O.; Olovsson, I. In *The Hydrogen Bond. Recent Developments in Theory and Experiments*; Schuster, P., Zundel, G., Sandorfy, C., Eds.; North-Holland: Amsterdam, 1976; Chapter 10, p 471.
- (3) Yoon, Y. K.; Carpenter, G. *Acta Crystallogr.* **1959**, *12*, 17.
- (4) Lundgren, J.-O.; Olovsson, I. *Acta Crystallogr.* **1967**, *23*, 966.
- (5) Lundgren, J.-O.; Olovsson, I. *Acta Crystallogr.* **1967**, *23*, 971.
- (6) Taesler, I.; Lundgren, J.-O. *Acta Crystallogr.* **1978**, *B34*, 2424.
- (7) Schindler, T.; Berg, C.; Niedner-Schatteburg, G.; Bondybey, V. E. *Chem. Phys. Lett.* **1994**, *229*, 57.
- (8) Lee, S. C.; Kaplow, R. *Science* **1970**, *169*, 477.
- (9) Triolo, R.; Narten, A. H. *J. Chem. Phys.* **1975**, *63*, 3624.
- (10) Ohtomo, N.; Arakawa, K.; Takeuchi, M.; Yamaguchi, T.; Ohtaki, H. *Bull. Chem. Soc. Jpn.* **1981**, *54*, 1314.
- (11) Lee, H.-G.; Matsumoto, Y.; Yamaguchi, T.; Ohtaki, H. *Bull. Chem. Soc. Jpn.* **1983**, *56*, 443.
- (12) Kameda, Y.; Uemura, O. *Bull. Chem. Soc. Jpn.* **1992**, *65*, 2021.
- (13) Kameda, Y. *Bull. Chem. Soc. Jpn.* **1997**, submitted for publication.
- (14) Walrafen, G. E.; Chu, Y. C. *J. Phys. Chem.* **1992**, *96*, 9127.
- (15) Walrafen, G. E.; Chu, Y. C.; Carlon, H. R. In *Proton Transfer in Hydrogen-Bonded Systems*; Bountis, T., Ed.; NATO ASI Series 291; Plenum: New York, 1992; p 297.
- (16) Zundel, G. In *The Hydrogen Bond, Recent Developments in Theory and Experiments*; Schuster, P., Zundel, G., Sandorfy, C., Eds.; North Holland: Amsterdam, 1976; p 687.
- (17) Danninger, W.; Zundel, G. *J. Chem. Phys.* **1981**, *74*, 2769.
- (18) Librovich, N. B.; Sakun, V. P.; Sokolov, N. D. *Chem. Phys.* **1979**, *39*, 351.
- (19) Downing, H. D.; Williams, D. *J. Phys. Chem.* **1976**, *80*, 1640.
- (20) Giguère, P. A. *J. Chem. Ed.* **1979**, *56*, 571.
- (21) Giguère, P. A. *Chem. Phys.* **1981**, *60*, 421.
- (22) Librovich, N. B.; Sakun, V. P.; Sokolov, N. D. *Chem. Phys.* **1981**, *60*, 425.
- (23) Hertz, H. G.; Maurer, R. *Z. Phys. Chem. NF* **1983**, *135*, 107.
- (24) Dippel, T.; Kreuer, K. D. *Solid State Ionics* **1991**, *46*, 3.
- (25) Agmon, N. *Chem. Phys. Lett.* **1995**, *244*, 456.
- (26) Agmon, N. *J. Chim. Phys. (Paris)* **1996**, *93*, 1714.
- (27) Tuckerman, M.; Laasonen, K.; Sprick, M.; Parrinello, M. *J. Phys. Chem.* **1995**, *99*, 5749.
- (28) Bell, R. A.; Cristoph, G. G.; Fronczek, F. R.; Marsh, R. E. *Science* **1975**, *190*, 151.
- (29) Pauling, L. *The Nature of the Chemical Bond*, 3rd edition; Cornell University Press: Ithaca, NY, 1960.
- (30) Metz, R. B.; Kitsopoulos, T.; Weaver, A.; Neumark, D. M. *J. Chem. Phys.* **1988**, *88*, 1463.
- (31) Schindler, T.; Berg, C.; Niedner-Schattenburg, G.; Bondybey, V. E. *J. Phys. Chem.* **1995**, *99*, 12434.
- (32) Laasonen, K. E.; Klein, M. L. *J. Phys. Chem. A* **1997**, *101*, 98.
- (33) Scheiner, S. *J. Am. Chem. Soc.* **1981**, *103*, 315.
- (34) Komatsuzaki, T.; Ohmine, I. *Chem. Phys.* **1994**, *180*, 239.
- (35) Desbat, B.; Huong, P. V. *Spectrochim. Acta* **1975**, *A31*, 1109.
- (36) Frisch, M. J.; DelBene, J. E.; Binkley, J. S.; Schaefer, H. F., III. *J. Chem. Phys.* **1986**, *84*, 2279.
- (37) Xie, Y.; Remington, R. B.; Schaefer, H. F., III. *J. Chem. Phys.* **1994**, *101*, 4878.
- (38) Pings, C. J. In *Physics of Simple Liquids*; Temperley, H. N. V., Rowlinson, J. S., Rushbrooke, G. S., Eds.; North-Holland: Amsterdam, 1968; Chapter 10, p 387.
- (39) James, R. W. *The Crystalline State*; Bell and Sons: London, 1950; Vol. II (*The Optical Principles of the Diffraction of X-Rays*); Chapter 9.
- (40) Narten, A. H.; Danford, M. D.; Levy, H. A. *Discuss. Faraday Soc.* **1967**, *43*, 97.

- (41) Prins, J. A.; Petersen, H. *Physica* **1936**, 3, 147.
(42) Morgan, J.; Warren, B. E. *J. Chem. Phys.* **1938**, 6, 666.
(43) Coulson, C. A.; Rushbrooke, G. S. *Phys. Rev.* **1939**, 56, 1216.
(44) Frenkel, J. *Kinetic Theory of Liquids*; Dover: New York, 1955.
(45) Wei, D.; Salahub, D. R. *J. Chem. Phys.* **1994**, 101, 7633.
(46) Wei, D.; Salahub, D. R. *J. Chem. Phys.* **1997**, 106, 6086.
(47) Agmon, N. *J. Mol. Liq.* **1997**, 73/74, 513.
(48) Andreani, C.; Ricci, M. A.; Nardone, M.; Ricci, F. P.; Soper, A. K. *J. Chem. Phys.* **1997**, 107, 214.
(49) Almlöf, J. *J. Mol. Struct.* **1981**, 85, 179.
(50) Lee, E. P. F.; Dyke, J. M. *Mol. Phys.* **1991**, 73, 375.
(51) Ando, K.; Hynes, J. T. *J. Mol. Liq.* **1995**, 64, 25.
(52) Gauduel, Y.; Pommeret, S.; Migus, A.; Yamada, N.; Antonetti, A. *J. Am. Chem. Soc.* **1990**, 112, 2925.